DOI: 10.13009/EUCASS2025-495
11TH EUROPEAN CONFERENCE FOR AERONAUTICS AND SPACE SCIENCES (EUCASS)

IMPACT OF ENGINE CYCLES, PROPELLANTS AND RECOVERY METHODS ON THE LAUNCH EXHAUST PROFILE OF REUSABLE BOOSTER STAGES

Moritz Herberhold, Jascha Wilken* and Martin Sippel**
** Space Launcher Systems Analysis, Institute of Space Systems, German Aerospace Center (DLR)*
Robert-Hooke-Straße 7, 28359 Bremen, Germany
Moritz.Herberhold@dlr.de – Jascha.Wilken@dlr.de – Martin.Sippel@dlr.de

Abstract
The rapid growth of spaceflight is driven by new engine cycles, propellant combinations, and recovery methods, enabling a new era of reusable launch systems. At the same time, there is an increasing effort to assess the environmental impact of spaceflight. Especially the emissions during the launch itself are a focus of the research, as they are essential to assess the effects of spaceflight on atmospheric chemistry, ozone depletion, and climate change.

This study combines these two developments by investigating the impact of engine cycles, propellants, and recovery methods on launch exhaust. The paper analyzes exhaust species, quantity, and distribution generated by different propulsion technologies, including staged combustion and gas-generator cycles, as well as propellants such as LOX-LCH$_4$, LOX-RP-1, and LOX-LH$_2$. Additionally, the study examines how first-stage recovery methods influence the overall exhaust profile, comparing vertical takeoff, vertical landing (VTVL) and vertical takeoff, horizontal landing (VTHL) approaches with expendable reference configurations. The European Next Reusable Ariane (ENTRAIN) reusable booster configurations developed by the German Aerospace Center (DLR) are used as case studies, as they are designed for the same use case, of transporting 7.5t of payload to GTO, allowing direct on-par comparison of the exhaust. Furthermore, they directly provide the detailed aerodynamic, mass and propulsion models, that are needed for the simulation of the exhaust profile generated during ascent and booster return.

The investigation of spaceflight's direct atmospheric impact is still at an early stage. Many phenomena like the creation of soot and the post-combustion between the exhaust and surrounding atmosphere are still largely unknown and the exact effects of many emissions into the high atmosphere stay highly debated. The DLR S3D initiative is currently researching these fields and develops and expands climate and post-combustion models that will be shown in later publications. By estimating key pollutants such as CO_2, H_2O and soot, for reusable launcher concepts this study provides valuable first insights into the trade-offs between performance, reusability, and environmental emissions.

1 Introduction

As reusable launch vehicles (RLVs) become a central focus of global aerospace development, understanding their environmental impact is increasingly critical. The benefits of reusability, including cost reduction and resource efficiency, are well-established. [1–4] However, the environmental footprint of these systems, particularly their emissions during launch and recovery, remains an area of active research [5–9].

One of the factors influencing the environmental impact of a launch is the exhaust profile generated by the rocket launch. [5, 9, 10] This profile describes the distribution and composition of the launch exhaust and is determined by a combination of factors, including the engine cycle, the choice of propellants, and the recovery method. Different engine cycles, such as gas generator (GG) and staged combustion (SC), produce varying exhaust species and quantities. Similarly, the choice of propellants, such as liquid oxygen-liquid hydrogen (LOX-LH$_2$), liquid oxygen-liquid methane (LOX-LCH$_4$), and liquid oxygen-kerosene (LOX-RP-1), directly affects the nature of the exhaust. These propellant

DOI: 10.13009/EUCASS2025-495

combinations have different combustion characteristics, leading to varying emissions of key species such as carbon dioxide (CO_2), water vapor (H_2O), and soot.

Additionally, the method of recovering the first stage of the launch vehicle can further alter the exhaust profile. Vertical takeoff, vertical landing (VTVL) approaches, as employed by SpaceX's Falcon 9 [11], rely on retro-propulsion for descent, generating additional exhaust during landing. In contrast, vertical takeoff, horizontal landing (VTHL) methods, such as the In-Air Capturing (IAC) concept studied by the German Aerospace Center (DLR) in the ENTRAIN program, avoid the need for descent propulsion, resulting in a different exhaust profile.

The ENTRAIN study [1–4, 12, 13], conducted by DLR, provides a comprehensive set of reusable and expandable configurations designed to explore these factors. Developed as part of a broader investigation into European reusable launch systems, the ENTRAIN configurations include ELV, VTVL, and VTHL concepts with a range of propellant combinations and engine cycles. These configurations offer a unique opportunity to conduct a direct comparative analysis of the exhaust of different booster concepts., as all of these are designed for the same mission of transporting 7.5 t to GTO.

This paper aims to investigate the impact of engine cycles, propellants, and recovery methods on the launch exhaust profile of reusable booster stages, using the ENTRAIN configurations as case studies. By examining the exhaust generated during ascent and recovery, this study seeks to provide insights into the trade-offs between performance, reusability, and generated exhaust. The findings are intended to support the development of future European launch systems and quantify the exhaust to aid further investigations into its environmental impact. The DLR S3D initiative is currently researching these fields and develops and expands climate and post-combustion models that will be shown in later publications.

However, it is important to note that this analysis is subject to several limitations. Foremost only the nozzle plane engine exhaust is modelled. The exhaust interactions with the atmosphere, including post-combustion processes and chemical transformations, are not modelled. Furthermore, the modeling assumes steady-state engine operation and does not account for transient phases such as ignition or throttling. The environmental impact of the exhaust is not assessed, and the results should be interpreted as an inventory of exhaust rather than a full environmental evaluation.

2 ENTRAIN study

The ENTRAIN study investigated and compared VTVL and VTHL launchers. A technical description of the VTVL and VTHL launchers can be found in [2, 3]. The propulsion datasets are discussed in [12]. The cost of the configurations and additional reference ELV launchers were investigated in [1]. A sketch of some of the investigated launchers is shown in Figure 1. An overview about the technical and performance parameters of all ENTRAIN launchers investigated in this paper is shown in Appendix A.

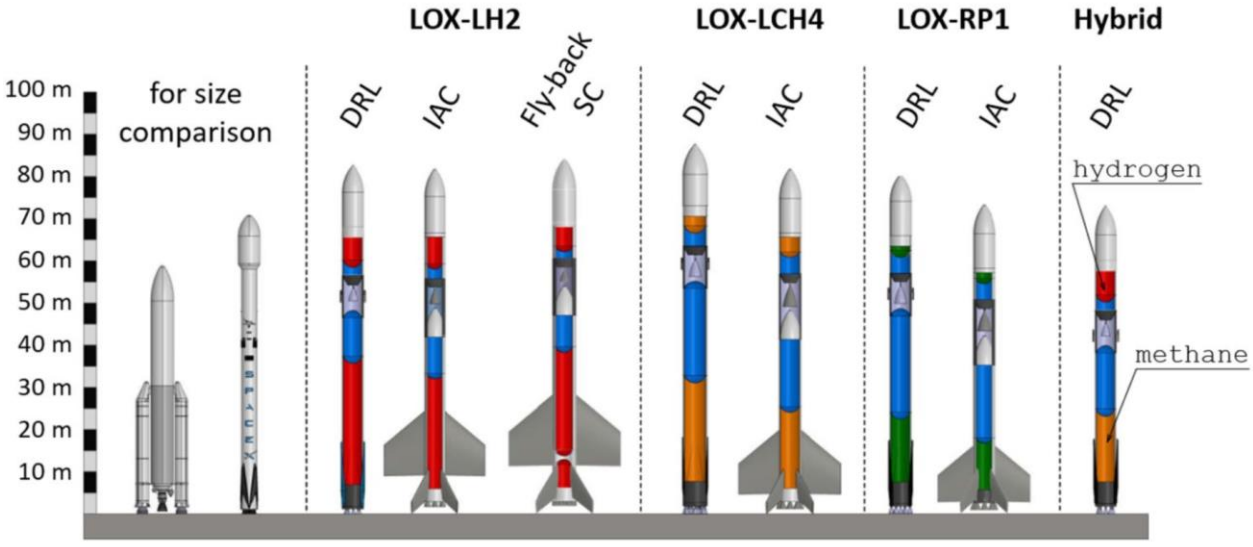

Figure 1: Sketch of selected launchers investigated within the ENTRAIN study, from Ref. [13]

DOI: 10.13009/EUCASS2025-495

2.1 Nomenclature

Due to the wide range of launchers considered in the ENTRAIN study a fixed nomenclature is used to distinguish the individual configurations based on key design parameters. The nomenclature is outlined in

Table 1. It uses simple abbreviations for the return method and engine cycle and a code of one letter per stage indicates the propellant combination of each stage. Finally, a code for the total Δv of the second stage is given. As an example, the code DRL CH SC Med describes a launcher that lands vertically downrange, uses staged combustion engines, LOX-LCH_4 in the first stage and LOX-LH_2 in the second stage and has a second stage total Δv of 7 km/s.

Table 1: ENTRAIN nomenclature abbreviations

Design parameter	Description	Nomenclature
Return Method	VTVL downrange landing	DRL
	VTHL in-air capturing	IAC
	None/Expendable	ELV
Propellant	LOX-LH_2	H
	LOX-LCH_4	C
	LOX-RP1	K
Engine cycles	Staged combustion	SC
	Gas generator	GG
Upper Stage Δv	7.0 km/s	Med

2.2 Study Overview

To interpret and compare the later discussed exhaust profiles of selected ENTRAIN configurations, first a short overview of the study logic and results central to this paper is necessary. The ENTRAIN study is characterized by a comparative approach. Identical modelling tools as well as identical high-level requirements and assumptions are used to ensure uniformity of the configurations Specifically, all configurations are two-stage launch vehicles designed to deliver a payload of 7.5 metric tons to Geostationary Transfer Orbit (GTO) from the Centre Spatial Guyanais (CSG) in Kourou. The configurations utilize the same propellant combinations in both stages—except for a single hybrid variant—and are equipped with the same engines, differing only in nozzle extension ratios. Overall, this ensures that differences in performance, mass, and exhaust can be attributed directly to the design choices rather than external factors.

This analysis limits itself to the following three degrees of freedom explored in the ENTRAIN study:

- Engine cycles:
  - Gas generator (GG)
  - Staged combustion (SC)
- Recovery modes:
  - VTVL with retropropulsion landing on downrange barge (DRL)
  - VTHL with in-air-capturing and subsequent towing by a waiting aircraft (IAC)
  - Expendable rocket without recovery (ELV)
- Propellant combinations:
  - Liquid oxygen (LOX)-Liquid Hydrogen (LH_2)
  - LOX-liquid Methane (LCH_4)
  - LOX-kerosene, rocket propellant-1 (RP-1)

The complete study also explored the second stages total Δv and additional propellants and recovery modes.

To give an overview over the results of the ENTRAIN study the dry mass and fuel mass of all configurations explored in this study are given in Figure 2 and Figure 3. In the ENTRAIN study, the impact of engine cycle choice was found to be most significant in hydrocarbon-fueled configurations. For LOX-LCH_4 systems, switching from GG to SC provided a noticeable gain in performance due to improved specific impulse, which translated to lower propellant mass and better overall efficiency. In contrast, for LOX-LH_2 systems, where specific impulse is already high, the relative advantage of SC over GG was smaller. However, SC engines also come with added complexity, contributing to higher engine dry mass.

DOI: 10.13009/EUCASS2025-495

Propellant choice was shown to be a dominant driver of both vehicle architecture and mass properties. The propellant density, and performance directly impacted structural mass and system sizing. LOX-LH_2 configurations benefited from the highest specific impulse, resulting in the lightest vehicles. But, they suffered from the lowest propellant density, resulting in large tank volumes and higher dry mass ratio, especially in the first stage. LOX-RP-1, by contrast, allowed for the most compact and lightweight tank structures due to its high density, but its lower efficiency required greater propellant masses and larger engines and produced the heaviest overall vehicles. LOX-LCH_4 was investigated as a compromise solution, offering moderate density and good specific impulse. However, the expected structural advantages of methane did not consistently materialize in the ENTRAIN configurations. Although the methane stages achieved lower dry mass ratios than their hydrogen equivalents, their Gross Lift Off Mass (GLOM) where always more than doubled. Especially GG LOX-LCH_4 stages were only small improvements compared to their LOX-RP-1 equivalents. A hybrid configuration using a LOX-LCH_4 first stage and a LOX-LH_2 upper stage achieved a competitive total mass by combining the higher density of methane in the lower stage with the high efficiency of hydrogen in the upper stage.

The ENTRAIN study found that ELV configurations had the lowest dry and fuel mass, as they required no recovery hardware or return manoeuvres—but came with the highest recurring costs due to stage loss. VTVL configurations with DRL added landing legs, grid fins, and significant return propellant, increasing both dry and fuel mass. Despite this, DRL achieved a high overall cost-efficiency, balancing reusability and performance. VTHL stages with IAC avoided return propellant, lowering fuel mass relative to DRL, but required wings, control surfaces, and landing gear, resulting in the highest dry mass. Additionally, IAC introduced higher non-recurring costs due to system complexity and support infrastructure, making it slightly less cost-effective than DRL despite its lower fuel demand.

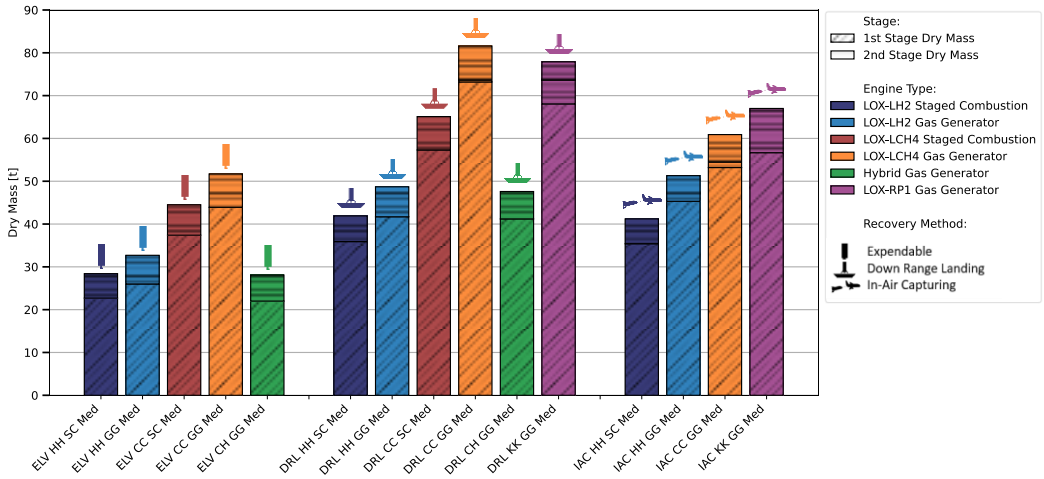

Figure 2: Dry mass of selected ENTRAIN configurations with different propellant combinations, engine cycles, and first stage recovery methods [1–3, 14]

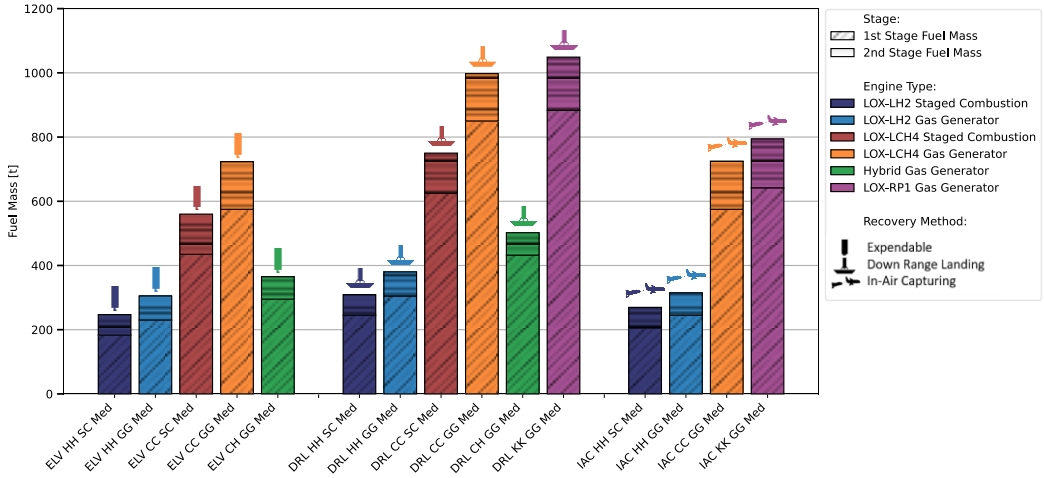

Figure 3: Fuel mass of selected ENTRAIN configurations with different propellant combinations, engine cycles, and first stage recovery methods [1–3, 14]

DOI: 10.13009/EUCASS2025-495

3 Exhaust modeling

A stepwise visualization of the exhaust modeling process is shown in Figure 4. Starting point of the exhaust modeling is the trajectory data from the ENTRAIN study. For each configuration a LEO, SSO, and GTO trajectory was created. The trajectories were optimized for maximum payload using the DLR internal trajectory optimizer TOSCA [15]. Amongst other parameters this trajectory data provides the rockets position, velocity, and heading, as well as the propellant mass flow rate for each engine type. The data along the trajectory is not continuous, instead it is given for distinct points with varying time intervals. In the early ascent many points with short time intervals are given to capture the dynamics of the acting aerodynamic forces, at higher altitudes the datapoints become less frequent with up to ten seconds and dozens of kilometers in-between each one.

Starting point of the exhaust modeling is the trajectory data from the ENTRAIN study. For each configuration a LEO, SSO, and GTO trajectory was created. The trajectories were optimized for maximum payload using the DLR internal trajectory optimizer TOSCA [15]. Amongst other parameters this trajectory data provides the rockets position, velocity, and heading, as well as the propellant mass flow rate for each engine type. The data along the trajectory is not continuous, instead it is given for distinct points with varying time intervals. In the early ascent many points with short time intervals are given to capture the complexity of the acting aerodynamic forces, at higher altitudes the datapoints become less frequent with up to ten seconds and dozens of kilometers in-between each one.

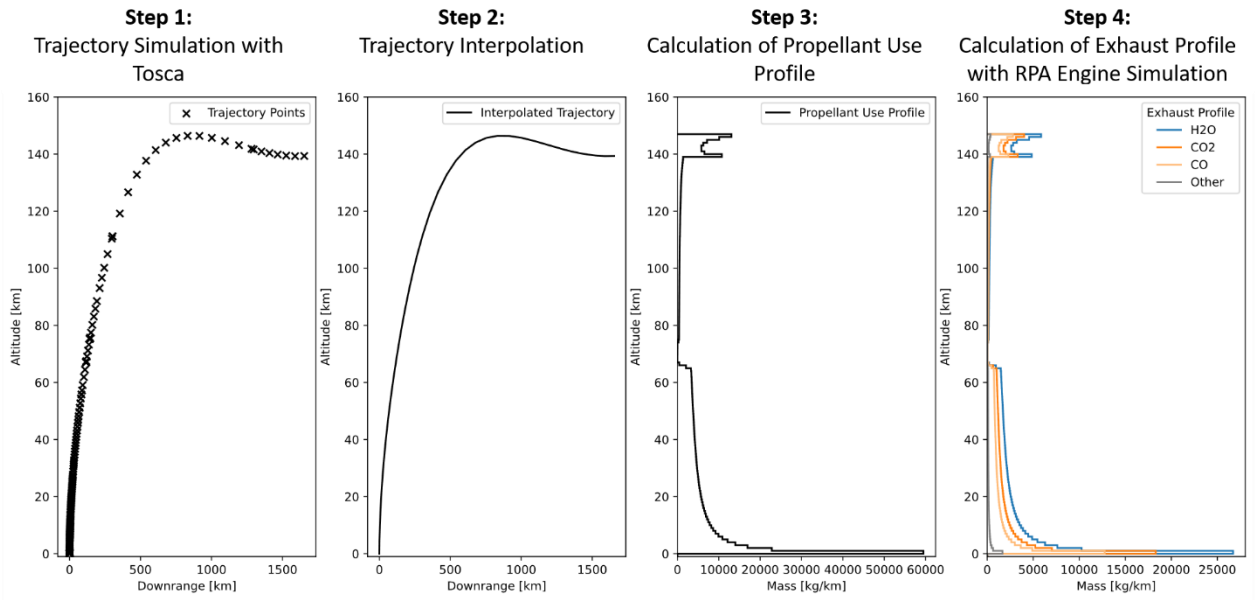

Figure 4: Stepwise visualization of the exhaust modeling process

A higher temporal resolution is necessary to accurately capture the dynamics of the propellant usage profile. Additionally, employing uniform time intervals significantly simplifies the numerical computation. To meet these requirements, the trajectory data is interpolated to a uniform time grid with intervals shorter than one millisecond. Based on the engine's mass flow rate and the fixed time step, the propellant consumption is computed for each data point. These data points are then grouped into bins and aggregated. In this study, one-dimensional altitude bins with a resolution of one kilometer are used to derive the altitude-dependent distribution of propellant usage. However, binning in two dimensions (typically altitude and downrange distance) or three dimensions (typically altitude, latitude, and longitude) is also possible. The result of this step is the exact amount of fuel used in each one-kilometer altitude band.

DOI: 10.13009/EUCASS2025-495

To calculate the exhaust resulting from the combustion of this fuel the commercial engine cycle analysis tool RPA [16] is used. RPA was already used to design the engines of the ENTRAIN configurations and detailed descriptions of the engine models can be found in [12]. In addition to the engine performance parameters the RPA calculations provide the mass wise chemical composition of the engine exhaust in the nozzle exit plane. For the analysis of the chemical reactions during the nozzle expansion three models can be chosen in RPA [17, 18]:

1. Frozen equilibrium after the nozzle throat. This usually underestimates the performance.
2. Shifting equilibrium throughout the nozzle. This usually overestimates the engines performance.
3. A combination of the first two approaches with a suddenly frozen flow. From the combustion chamber injector face to a predefined station in the expanding nozzle a shifting equilibrium is assumed. After that station a frozen equilibrium is assumed up to the nozzle exit. The position of the “frozen station” can either be defined by an area ratio or pressure ratio. The performance of this approach can be adjusted with these ratios. For each propellant combination a different empiric ratio is used to achieve a realistic engine performance estimation.

For the engine performance estimation in the ENTRAIN study [12], as well as for the exhaust calculations presented in this work, the third approach is employed. The selected area ratio for the so-called "frozen station" is based on empirical values reported in [18]. It should be emphasized that these values and the modeling approach are chosen to realistically represent engine performance, the modeling approach and area ratio required for an accurate representation of the exhaust composition may differ. To gain deeper insight, future validation studies based on experimental data or complex numerical simulations are required.

All engines are simulated in steady-state operation at 100% thrust. This represents only a minor simplification, as throttling in the ENTRAIN study is applied solely during the final seconds of the landing burn for vertically landing booster stages. During all other flight phases, the engines operate either at full thrust or are completely shut down. Transition processes such as ignition, ramp-up, and shutdown are not modelled.

For gas generator cycle engines, a second RPA model is employed to simulate the fuel-rich exhaust from the gas generator. The emission indexes from the gas generator and the main combustion chamber are combined proportionally based on their respective mass flow rates. In the case of hydrocarbon-combustions under fuel-rich conditions—as in the LOX-LCH$_4$ and LOX-RP1 engine’s gas generators—the RPA simulations indicate the formation of elemental carbon (graphite) as a reaction product. For the LOX-RP1 gas generator engine, the calculated carbon emission index of ~ 40 g/kg is comparable to the 25 g/kg of the Atlas II LOX-RP1 gas generator engine reported in [7]. RPA does not provide further details regarding the formation mechanisms, size, or morphology of resulting carbon particles.

It is important to note, that post-combustion of the highly energetic exhaust after the nozzle exit and reactions with the surrounding atmosphere are not represented in this study. All emission indexes used, describe the state of the exhaust at the engine’s nozzle exit. Further limitations of this study are discussed in section 5.4.

4 Results

This chapter present the results of the exhaust calculations and gives a short overview about the major trends. A more detailed discussion and comparison of the exhaust profiles, compositions, and amounts follows in chapter 5.

In this study the exhaust composition and distribution of 15 ENTRAIN configurations is calculated. The study focuses on the H_2O, CO_2, CO, CH_4 and elemental carbon exhaust. All other exhaust products are given in the detailed exhaust tables but are summarized in the plots and discussions as others The detailed results for the five ELV configurations are shown in Table 2, for six DRL configurations in Table 3 and for the four IAC configurations in Table 4. A visualization of the results is given in Figure 5. The exhaust of all configurations is calculated for a launch into GTO from Kourou. To ensure a proper alignment of the GTO’s apogee with the geostationary orbit a second manoeuvre after the initial ascent is necessary. In the optimization of the initial ascent, propellant is reserved for this second manoeuvre, but the second manoeuvre is not directly modelled as part of the ascent trajectory. Therefore, the total amount of propellant used in the initial ascent and with that the total exhaust mass created, is lower than the total amount of propellant of the configurations listed in Table 6, Table 7 and Table 8.

DOI: 10.13009/EUCASS2025-495

Table 2: Total Exhaust mass by exhaust species of selected ELV ENTRAIN configurations with different propellant combinations, engine cycles

Exhaust species	-	ELV HH SC Med	ELV HH GG Med	ELV CC SC Med	ELV CC GG Med	ELV CH GG Med
Total	[kg]	232384	289137	537481	696533	351040
H_2O	[kg]	222570	268863	241524	296447	178570
CO_2	[kg]	-	-	165552	217597	91596
CO	[kg]	-	-	115440	117610	49507
CH_4	[kg]	-	-	-	38105	16040
OH	[kg]	4030	4846	7959	12410	6194
H_2	[kg]	4918	14386	4078	3794	4475
Carbon	[kg]	-	-	-	3268	1376
O_2	[kg]	569	684	2278	6122	2714
O	[kg]	140	168	433	908	416
H	[kg]	158	190	209	260	147
HO_2	[kg]	2	2	7	12	6
H_2O_2	[kg]	1	1	2	3	2
COOH	[kg]	-	-	3	3	2
HCO	[kg]	-	-	2	2	1
HCOOH	[kg]	-	-	1	1	1
C_2H_6	[kg]	-	-	-	1	1
HCHO	[kg]	-	-	1	0	0

Table 3: Total Exhaust mass by exhaust species of selected DRL ENTRAIN configurations with different propellant combinations, engine cycles

Exhaust species	-	DRL HH SC Med	DRL HH GG Med	DRL CC SC Med	DRL CC GG Med	DRL CH GG Med	DRL KK GG Med
Total	[kg]	295628	365176	743973	973243	492757	1028779
H_2O	[kg]	283144	339569	334313	414216	238880	259524
CO_2	[kg]	-	-	229154	304040	135872	327053
CO	[kg]	-	-	159790	164332	73438	310872
CH_4	[kg]	-	-	-	53243	23794	33080
OH	[kg]	5126	6120	11017	17340	8719	28005
H_2	[kg]	6256	18170	5644	5300	5246	8729
Carbon	[kg]	-	-	-	4567	2041	41343
O_2	[kg]	723	863	3153	8554	3959	15624
O	[kg]	178	213	599	1269	601	3763
H	[kg]	201	240	288	363	200	699
HO_2	[kg]	2	3	9	16	8	-
H_2O_2	[kg]	1	1	3	4	2	-
COOH	[kg]	-	-	4	4	2	-
HCO	[kg]	-	-	3	2	1	-
HCOOH	[kg]	-	-	2	1	1	-
C_2H_6	[kg]	-	-	-	1	1	-
HCHO	[kg]	-	-	1	0	0	-

DOI: 10.13009/EUCASS2025-495

Table 4: Total Exhaust mass by exhaust species of selected IAC ENTRAIN configurations with different propellant combinations, engine cycles

Exhaust species	-	IAC HH SC Med	IAC HH GG Med	IAC CC GG Med	IAC KK GG Med
Total	[kg]	257418	301864	703495	761864
H_2O	[kg]	246547	280698	299410	192191
CO_2	[kg]	-	-	219772	242200
CO	[kg]	-	-	118785	230217
CH_4	[kg]	-	-	38486	24497
OH	[kg]	4464	5059	12534	20739
H_2	[kg]	5448	15020	3832	6465
Carbon	[kg]	-	-	3301	30617
O_2	[kg]	630	714	6183	11570
O	[kg]	155	176	917	2787
H	[kg]	175	198	262	518
HO_2	[kg]	2	2	12	-
H_2O_2	[kg]	1	1	3	-
COOH	[kg]	-	-	3	-
HCO	[kg]	-	-	2	-
HCOOH	[kg]	-	-	1	-
C_2H_6	[kg]	-	-	1	-
HCHO	[kg]	-	-	0	-

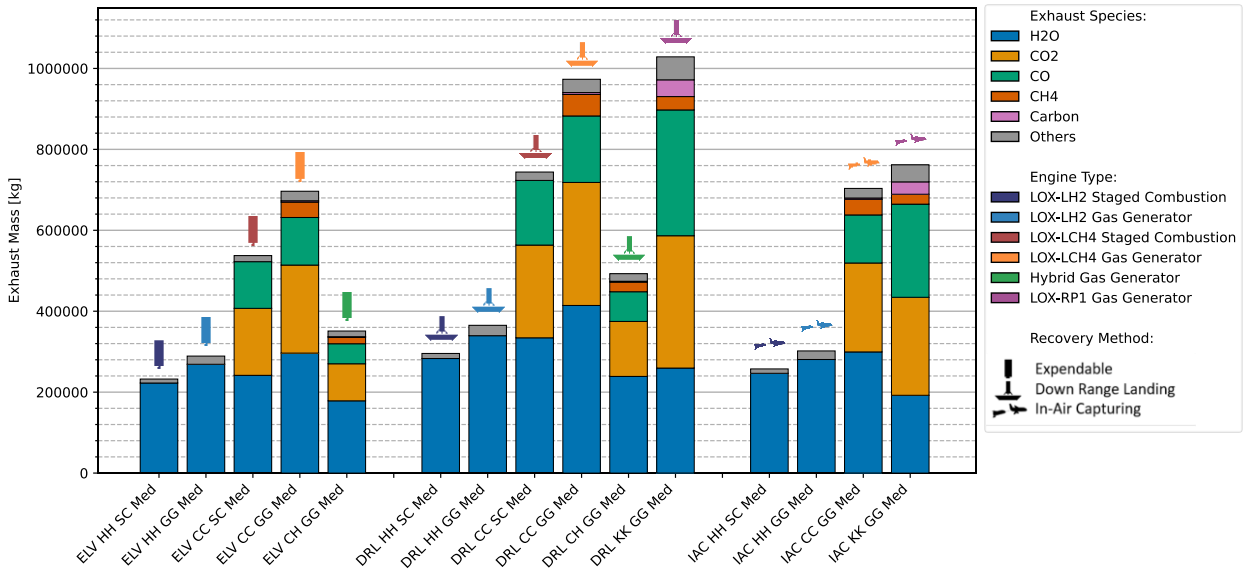

Figure 5: Total Exhaust mass by exhaust species of selected ENTRAIN configurations with different propellant combinations, engine cycles, and first stage recovery methods

For a short summary of the results, Figure 3 shows the total exhaust and its composition for each configuration. The calculated exhaust compositions reveal clear trends linked to propellant choice, engine cycle, and recovery method. LOX-LH_2 configurations consistently produce the least total exhaust mass, dominated by water vapor (H_2O). In contrast, hydrocarbon-based configurations (LOX-LCH_4 and LOX-RP-1) show significantly higher exhaust masses that include CO_2, CO, and elemental carbon. The LOX-LCH_4 configurations even exhaust more water vapor than their LOX-LH_2 counterparts. LOX-RP-1 generates the highest total exhaust and the highest amount of carbon. The hybrid CH configurations—combining methane in the first stage with hydrogen in the second—strike a middle ground,

DOI: 10.13009/EUCASS2025-495

showing reduced CO_2 and CO exhaust compared to full-hydrocarbon designs but larger total exhaust than the full-hydrogen designs. The use of staged combustion engines over gas generator engines consistently reduces the total exhaust and for LOX-LCH_4 engines it also reduces the release of elemental carbon and methane
The booster recovery method also impacts the total exhaust. ELV launchers have the lowest overall exhaust mass due to the absence of recovery burns and recovery hardware. DRL configurations show the highest total exhaust, driven by the need for return propellant and additional landing hardware. IAC designs fall in between, avoiding return burns but incurring higher dry mass due to wings and control systems.

5 Discussion

The following chapter provides an in-depth analysis of the exhaust inventories as well as a discussion of the exhaust's altitude distribution. Main focus of the discussion are the impact of the engine cycle, propellant and recovery method, but first a general discussion of the exhaust distribution is given.

Figure 6 shows the altitude-wise exhaust distribution, the ascent trajectory and the exhaust composition for a GTO launch of the DRL CC GG configuration. The exhaust generated during the ascent is shown as a solid line in the left plot and the additional exhaust created by the booster descent is shown by the dashed line. The altitude-wise exhaust distributions of all shown configurations follow a similar pattern. At ground level the largest exhaust concentration can be found, as the rocket spends the longest time in the initial kilometer. As the launcher builds up more and more vertical velocity it spends less time in each altitude band and leaves less exhaust. With increasing altitude, the ascent becomes more horizontal and the vertical velocity and with it the exhaust per kilometer level out, until the point of stage separation is reached. Overall the first stage's exhaust profile can be described by a decay curve, which decays to a constant non-zero value.

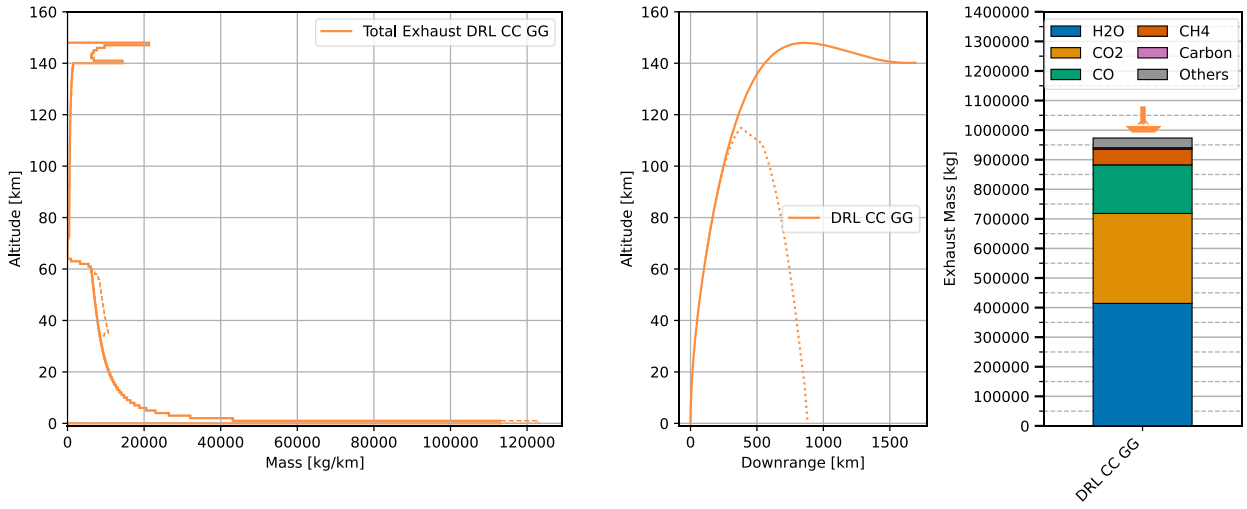

Figure 6: Exhaust inventory of the ENTRAIN DRL CC GG launcher; Left: Total exhaust mass distributions over altitude, the dashed line shows the exhaust generated during the recovery of the DRL first stage; Middle: Ascent trajectory, with the DRL booster return trajectory as dotted line; Right: Total exhaust masses by species

After stage separation the rocket continues its ascent for ten seconds without any active engine. In the exhaust profile this phase shows as a gap without exhaust. Now the second stage is ignited and due to its lower thrust and mass flow a considerably lower exhaust concentration is left. With the further levelling out of the trajectory the vertical velocity decreases and the exhaust per kilometer altitude starts to increase again. At the final altitude of the ascent two kinds of distributions form depending on the ascent trajectory. If the ascent trajectory does not overshoot the final altitude, the exhaust per kilometer continuously increase until it forms one peak at the final altitude. An example of this kind of distribution can be seen for the ELV HH GG configuration in Figure 8. If the ascent trajectory overshoots the final orbital altitude a distribution with two peaks forms, as shown in Figure 6. One peak is at the highest altitude of the ascent trajectory and the second is at the final altitude. In between these peaks a higher exhaust mass per kilometer altitude can be found as the launcher crosses these altitudes twice. This second distribution is more common in this study as most ENTAIN launchers have an overshooting ascent trajectory.

DOI: 10.13009/EUCASS2025-495

For the DRL configurations exhaust is also created during the descent of the first stage. This additional exhaust is marked by a dashed line, as seen in the left plot in Figure 6. First a re-entry burn is needed to decrease the thermal and aerodynamic loads during the re-entry. This burn usually occurs between 60 km and 30 km and increases the exhaust in this altitude band. The final landing burn of the booster also leaves additional exhaust at ground level.

To place the exhaust profile in context, Figure 7 compares results from two representative ENTRAIN configurations (ELV HH SC and DRL CC GG) with published data from Barker et al. [19], Ross et al. [20] and launch data extracted from a Falcon 9 Block 2 livestream, also reported by Barker et al. [19]. Overall, the profiles are in general agreement: all show the highest exhaust mass concentrated within the first five kilometers of altitude, followed by a continuous decline up to approximately 50 km. This behavior is consistent across both the ENTRAIN and reference profiles.

However, notable differences emerge due to the nature of the data. The profiles presented in this study are derived from individual launch vehicle configurations, whereas the Ross and Barker profiles represent averages over multiple launchers. As such, a certain degree of variance is expected. For example, both the ENTRAIN launchers and the Falcon 9 livestream data exhibit a greater proportion of total propellant consumption within the first five kilometers compared to the averaged profiles. The DRL CC GG configuration also displays a distinct drop in exhaust mass at the stage separation altitude, in contrast to the smoother gradient observed in the Barker profile an effect that can also be attributed to averaging across launch vehicles with differing stage separation points. Additionally, the DRL CC GG profile uniquely captures the exhaust contributions from the re-entry and landing burns of its reusable booster. Interestingly, the Ross and Barker profiles show an unexpected increase in burned propellant above 50 km, a feature absent from both ENTRAIN and Falcon 9 data; the origin of this increase remains unclear.

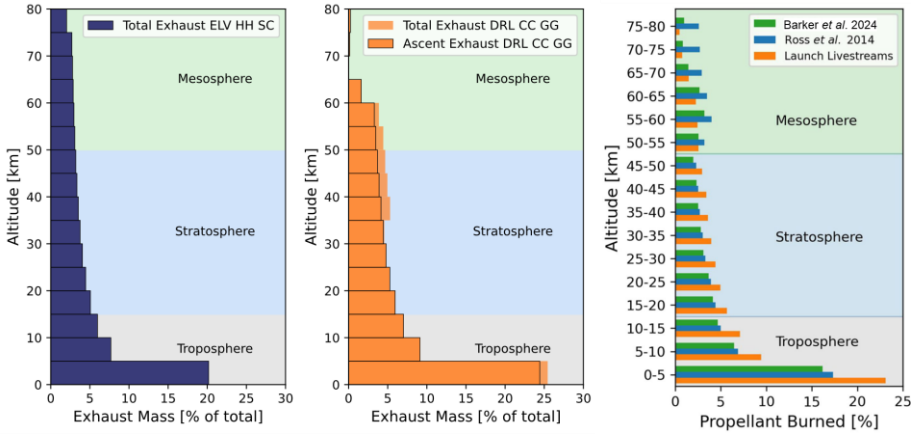

Figure 7: Comparison of the exhaust altitude profile of the ENTRAIN ELV HH SC configuration on the left and the ENTRAIN DRL CC GG configuration in the middle with literature distributions from Barker *et al.* [19] and Ross *et al.* [20] and a Falcon 9-2 launch livestream also taken from Barker *et al.* [19]. Shading distinguishes the troposphere (grey), stratosphere (blue), and mesosphere (green).

5.1 Impact of the engine cycle

The main impact of the engine cycle on the launch exhaust is an increase in total exhaust for equivalent GG configurations over SC configurations. The lower specific impulse (I_{sp}) of the gas generator engines, increases the total propellant mass needed to achieve the set mission of the ENTRAIN study and the exhaust increases proportionally. For the ELV configurations, as shown in Table 2, Figure 8, and Figure 9 this increases the total exhaust mass by 24% for the LOX-LH_2 configurations and by 29% for the LOX-LCH_4 configurations. Although the absolute improvement of the I_{sp} by using a SC cycle is roughly equivalent for both propellants [12], it yields a larger fuel mass reduction for the lower I_{sp}-regime of the LOX-LCH_4 engines [1, 2].

DOI: 10.13009/EUCASS2025-495

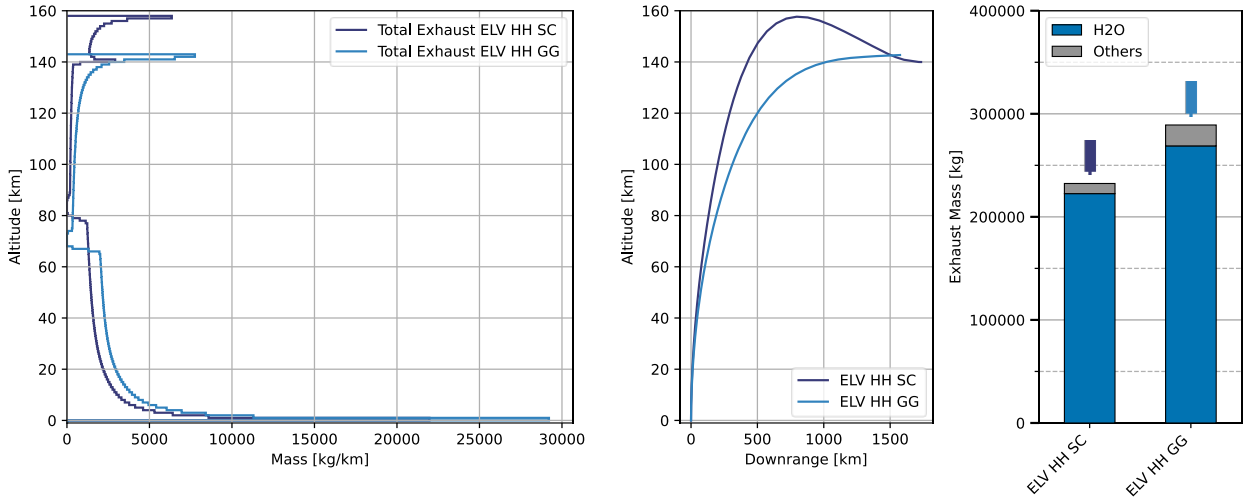

Figure 8: Comparison of the ENTRAIN ELV HH launchers with gas generator engines and staged combustion engines; Left: Comparison of total exhaust mass distributions over altitude; Middle: Comparison of the ascent trajectories; Right: Comparison of the total exhaust masses by species

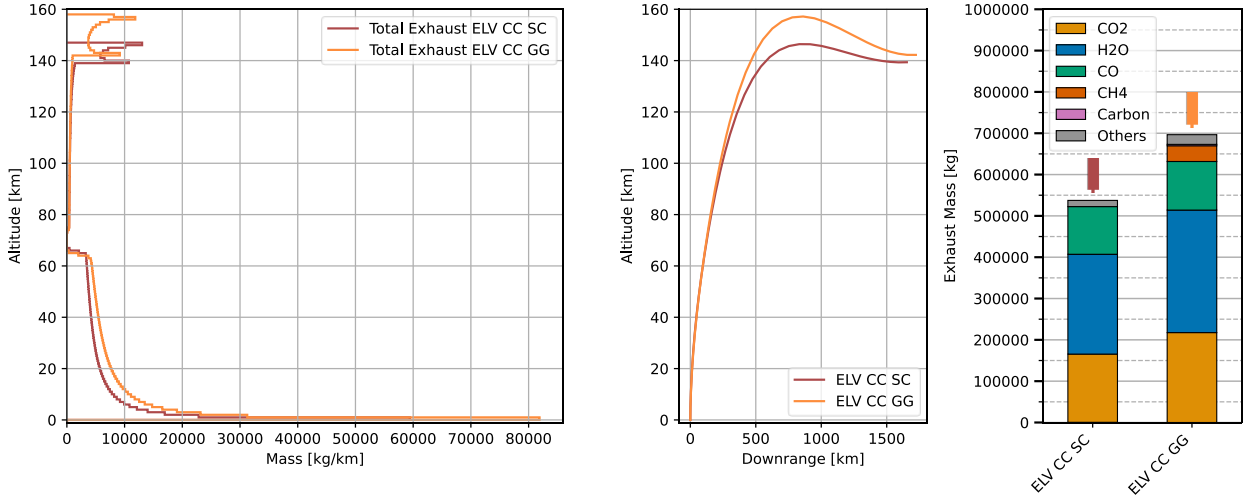

Figure 9: Comparison of the ENTRAIN ELV CC launchers with gas generator engines and staged combustion engines; Left: Comparison of total exhaust mass distributions over altitude; Middle: Comparison of the ascent trajectories; Right: Comparison of the total exhaust masses by species

Additionally, the engine cycle impacts the composition of the exhaust. Both engine cycles use a preburner to generate hot gas that powers the propellant turbopumps. They differ in how they handle the exhaust from the preburner: GG engines vent it overboard, while SC engines burn it fully in the main chamber for higher efficiency. Therefore, GG engines have a secondary exhaust flow, that can account for up to 10% of the total exhaust. In the ENTRAIN study all gas generators use a fuel rich mixture ratio [12].

For the LOX-LH_2 engines the gas generator mass flow rate is with ~4% of the total engine flow rate relatively low and the impact on the exhaust composition is limited. The total engine mixture ratio stays at six for both cycles. As listed in Table 5, the share of molecular hydrogen increases from 2% to 5% compared with the SC engine and the share of water decreases accordingly from 96% to 93%. All other combustion products show only minimal proportion changes. For LOX-LCH_4 engines the cycle impact on the exhaust composition is larger. The gas generator massflow accounts for 9% of the total mass flow and the total engine mixture ratio shifts significantly from 2.5 for the GG cycle to 3.25 for the SC cycle. This impacts the proportions of all exhaust species, as shown in Table 5. The most significant changes are, that the GG engine directly emits methane and elemental carbon as part of the fuel rich exhaust from the gas generator.

DOI: 10.13009/EUCASS2025-495

Table 5: Impact of the engine cycle on the exhaust composition for ENTRAIN LOX-LH_2 and LOX-LCH_4 engines

Exhaust species	-	LOX-LH_2 SC	LOX-LH_2 GG	LOX-LCH_4 SC	LOX-LCH_4 GG
H_2O	[%]	95,8%	93,0%	44,9%	42,6%
CO_2	[%]	-	-	30,8%	31,2%
CO	[%]	-	-	21,5%	16,9%
CH_4	[%]	-	-	-	5,5%
OH	[%]	1,7%	1,7%	1,5%	1,8%
H_2	[%]	2,1%	5,0%	0,8%	0,5%
Carbon	[%]	-	-	-	0,5%
O_2	[%]	0,2%	0,2%	0,4%	0,9%
O	[%]	0,1%	0,1%	0,1%	0,1%
H	[%]	0,1%	0,1%	0,0%	0,0%

Overall the comparison shows that the engine cycle has a relevant impact on the launch exhaust composition and quantity both for LOX-LH_2 launchers and LOX-LCH_4 launchers. The impact is bigger for the hydrocarbon rocket, as it causes a larger increase in the total exhaust mass, a larger impact in the exhaust composition and the creation of elemental carbon as one exhaust product. A direct impact of the engine cycle on the exhaust distribution is not observed. As this study and the ENTRAIN studies [1–4, 12, 13] show, the use of SC engines reduces the total launch exhaust, the launcher's dry mass, and fuel mass. Accordingly, a lower environmental impact of the fuel production, manufacturing, and launch emissions can be expected.

5.2 Impact of the propellant

Of all the design parameters investigated, the propellant choice exhibits the most significant influence on both the total quantity and chemical composition of the rocket exhaust. The three primary propellant combinations analyzed— LOX-LH_2, LOX-LCH_4, and LOX-RP-1—demonstrate substantial variation in exhaust mass and composition. Figure 10 and Figure 11 compare the exhaust distribution and composition for all four DRL GG configurations.

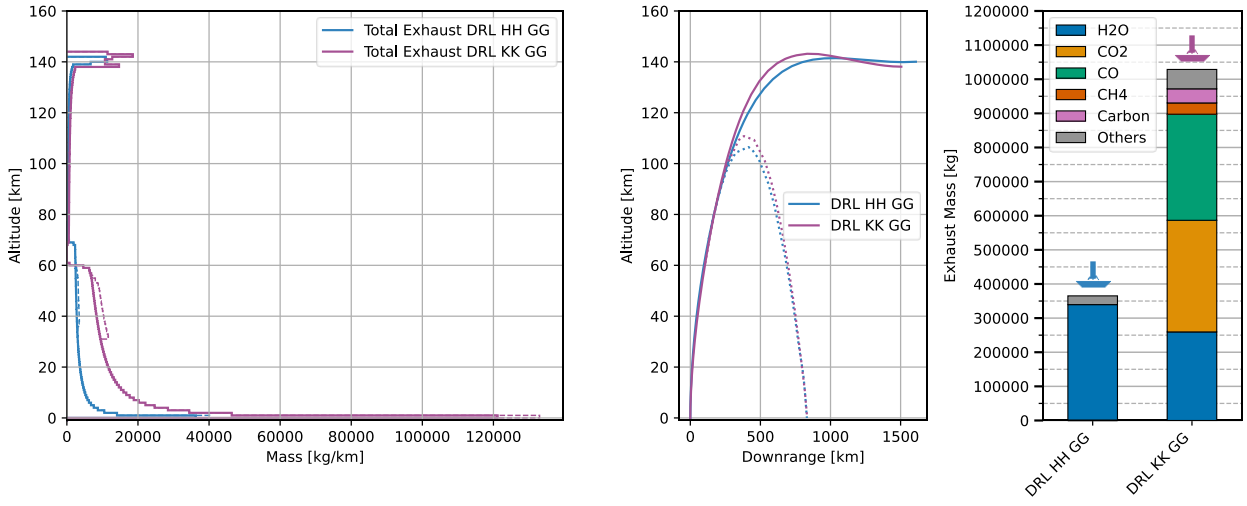

Figure 10: Comparison of the ENTRAIN DRL GG launchers with LOX-LH_2 and LOX-RP1 propellants; Left: Comparison of total exhaust mass distributions over altitude, the dashed line shows the exhaust generated during the recovery of the DRL first stage; Middle: Comparison of the ascent trajectories, with the DRL booster return trajectory as dotted line; Right: Comparison of the total exhaust masses by species

As shown in Chapter 4 and Figure 10 LOX-LH_2 configurations consistently produce the lowest total exhaust mass. Their exhaust is the "cleanest", with water vapor accounting for the vast majority of the exhaust, alongside small fractions of molecular hydrogen and hydroxyl species. No carbon-based compounds are formed, and no soot is

DOI: 10.13009/EUCASS2025-495

generated. In contrast, LOX-RP-1 configurations show with more than 1000 t the highest total exhaust mass and the most carbon-rich exhaust profile. The gas generator RP-1 launchers produce large quantities of carbon dioxide, carbon monoxide, and water vapor. With 4% of the total exhaust, they also create the largest amount of elemental carbon.

LOX-LCH_4 is often considered a compromise between hydrogen and kerosene, but the results of the ENTRAIN study and this study reveal that full methane configurations perform far closer to RP-1 than to hydrogen in terms of exhaust and performance. The methane launchers produce considerable amounts of H_2O, CO_2 and CO, and with GG engines also release unburned methane due to fuel-rich preburner exhaust. The methane launchers even emit more water vapor than the equivalent LOX-LH_2 launchers, therefore, a larger environmental impact of the launch emissions can be expected. Compared to the LOX-RP-1 configurations with the same engine cycle the total exhaust is only slightly reduced, but the amount of elemental carbon is reduced by a factor of nine. Although large uncertainties remain, many studies agree that black carbon is central to the overall environmental effect of launch emissions [5, 9, 20]. Accordingly, this substantial reduction of black carbon emissions might yield a substantial reduction of the environmental impact of the launch emissions. The LOX-LCH_4 SC configurations provide a significant reduction in total exhaust compared to LOX-RP1 GG and exhaust no elemental carbon, but as no LOX-RP1 SC configuration is investigated in this study no direct comparison is possible.

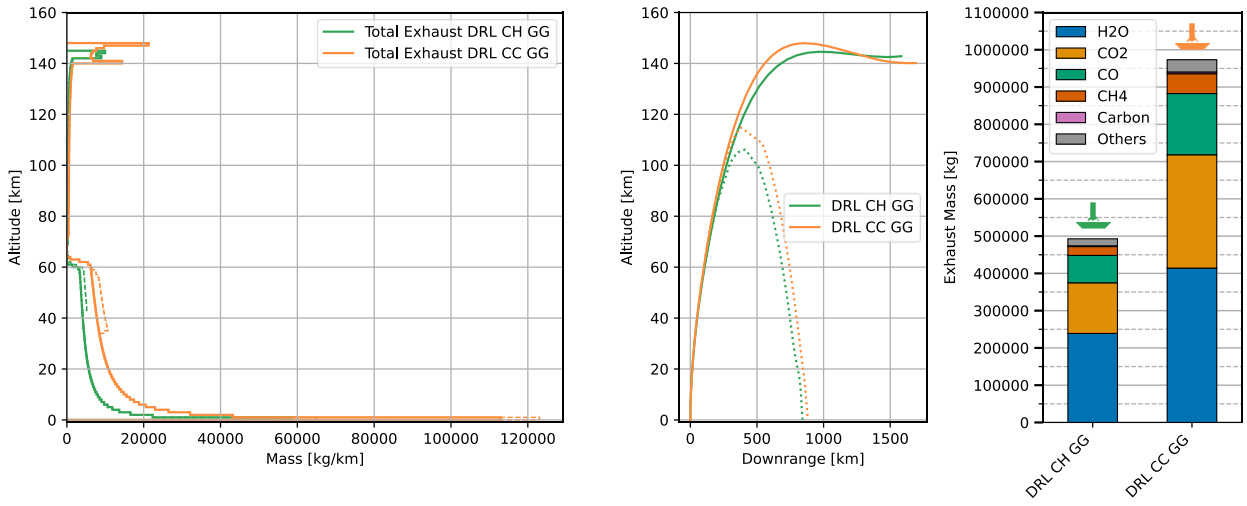

Figure 11: Comparison of the ENTRAIN DRL GG launchers with Hybrid and LOX-CH_4 propellants; Left: Comparison of total exhaust mass distributions over altitude, the dashed line shows the exhaust generated during the recovery of the DRL first stage; Middle: Comparison of the ascent trajectories, with the DRL booster return trajectory as dotted line; Right: Comparison of the total exhaust masses by species

The hybrid CH configuration, which uses LOX-LCH_4 in the first stage and LOX-LH_2 in the second, emerges as an effective compromise. This design combines the higher density and structural efficiency of methane for the booster with the high I_{sp} and low total mass of hydrogen for the upper stage. As a result, the CH configuration reduces overall CO_2, CO, CH_4, and elemental carbon exhaust by more than 50% compared to full hydrocarbon designs. Compared to the full hydrogen GG configurations the total exhaust mass increases by a third.

Although the propellant has significant impact on the total exhaust mass and its composition, no influence on the distribution of the exhaust can be found. Overall LOX-LH_2 launcher create the smallest and “cleanest” exhaust, whilst LOX-RP1 GG launchers generate the most and most carbon-rich exhaust, including significant amounts of elemental carbon. The LOX-LCH_4 GG configurations offer only a marginal reduction in total exhaust, although they reduce the elemental carbon by a factor of nine. The CH configurations provide a middle ground between the hydrocarbon and hydrogen configurations, both in exhaust amount and composition. Early studies on the environmental impact of launch vehicle emissions suggest that, for an equivalent mass of propellant, exhaust from hydrocarbon-fueled launchers may have an effect up to three orders of magnitude greater than hydrogen-fueled counterparts [21, 22]. When combined with the findings of this study—namely, that hydrocarbon configurations produce approximately three times more exhaust mass than hydrogen configurations—it can be expected that the use of hydrogen as a propellant offers a substantial reduction in the overall environmental impact of launch exhaust.

DOI: 10.13009/EUCASS2025-495

5.3 Impact of the recovery strategy

To compare the exhaust of the three investigated recovery strategies–ELV, DRL and IAC–the GTO trajectories, exhaust distributions and total exhaust masses are shown for all ENTRAIN HH SC configurations in Figure 12. As all configurations use identical engines, no impact on the exhaust composition can be seen, but impacts on the total exhaust mass and exhaust distribution are visible.

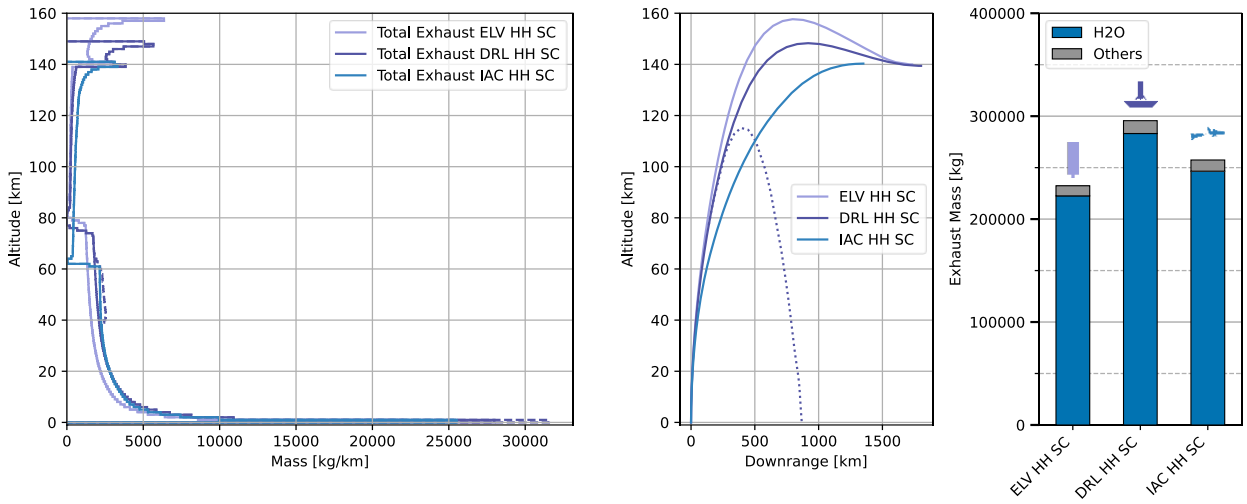

Figure 12: Comparison of the ENTRAIN GG LOX-LH_2 launchers with different first stage recovery methods; Left: Comparison of total exhaust mass distributions over altitude, the dashed line shows the exhaust generated during the recovery of the DRL first stage; Middle: Comparison of the ascent trajectories, with the DRL booster return trajectory as dotted line; Right: Comparison of the total exhaust masses by species; Colours not consistent with other plots to allow distinction of recovery methods

Compared to the ELV system the use of DRL recovery increases the total exhaust by 27%. This increase is caused by the increased Δv budget required for the re-entry-burn and landing burn of the DRL booster recovery and the additional hardware, like landing legs and aerodynamic control surfaces. The increase also depends on the I_{sp} of the engine cycle and propellant combination of the booster stage, as booster with lower I_{SP} need a larger additional fuel mass fraction to provide the additional Δv. For example, for the LOX-LCH_4 GG and hybrid GG configurations the total exhaust mass increases by 40% between the ELV and DRL configurations, as both use the same engine and propellant in the booster stage. For the IAC recovery the total exhaust only increases by 10% for the LOX-LH_2 SC configurations. For this recovery additional systems, like wings and landing gears are necessary but no additional engine burns and, therefore, no larger Δv budget. This results in a smaller increase of the total fuel mass and exhaust. Both booster recovery strategies require additional emissions by secondary vehicles, like the barge the DRL booster stage lands on or the aircraft, that tows back the IAC booster stage. These are not part of this study but have to be taken in account for a realistic environmental impact estimation.

As illustrated in Figure 12, the recovery strategies influence the vertical exhaust distribution, due to the distinct booster trajectories associated with each strategy. The ELV and DRL boosters exhibit similar ascent profiles, characterized by steep trajectories and stage separation occurring at approximately 80 km altitude. However, the additional atmospheric re-entry burn and landing burn distinguish the DRL booster's trajectory. The re-entry burn adds exhaust between 60 km and 40 km and the final landing burn increases the exhaust at ground level. These two burns account for approximately 4% to 5% of the total exhaust. In contrast, the IAC recovery does not incorporate any post-separation engine burns. Instead, its booster follows a shallower ascent trajectory to mitigate thermal loads during aerodynamic re-. As a result, stage separation occurs at a lower altitude of around 60 km, leading to a more concentrated exhaust distribution within a narrower altitude range.

These findings highlight that the choice of recovery strategy introduces differences in both the magnitude and distribution of exhaust. While ELV configurations benefit from minimal complexity and the lowest total exhaust, they sacrifice reusability. DRL systems add substantial exhaust due to the required propulsive manoeuvres, with clear concentration in lower meso- and upper stratosphere and at ground level. IAC offers an intermediate solution, avoiding return propulsion and thus reducing the launch exhaust compared to DRL boosters. As such, the recovery method must be considered not only in terms of system architecture and operational cost but also as a factor shaping the propellant

DOI: 10.13009/EUCASS2025-495

usage and exhaust characteristics of reusable launch vehicles. Without a quantification of the impact of launch emissions it remains uncertain, how the increase in launch exhaust and fuel mass impacts the overall footprint of reusable systems.

5.4 Limitations

While this study provides a detailed and systematic assessment of launch exhaust across a wide range of configurations, several limitations should be noted. All engine simulations were conducted under steady-state conditions at full thrust. Transient phases such as ignition, ramp-up, shutdown, or throttled operations were not captured. Although these periods are typically brief, they may slightly alter the actual exhaust composition. The booster ascent is also at full thrust without throttling around the point of maximum dynamic pressure, which is very common in rocketry. Furthermore, all configurations were constrained to a GTO mission with 7.5 t payload and used common design assumptions. While this allows for a clean comparison, results are not directly transferable to other mission types or launcher designs.

The "frozen station" nozzle combustion approach described in section 3 is based on a realistic representation of the engine's performance and it is not given, that this approach or the chosen position of the "frozen station" also yield a realistic representation of the engine exhaust. Furthermore, the analysis considers exhaust species as they leave the nozzle exit and does not include post-combustion or interactions with the surrounding atmosphere. Effects such as soot oxidation, plume-atmosphere chemistry, or re-condensation of species are not modeled and could influence the final emissions. Elemental carbon is estimated based on equilibrium predictions from RPA under fuel-rich gas generator conditions but without resolving particle formation processes, morphology, or post-nozzle changes.

The spatial exhaust distribution is based on the altitude of exhaust only. The subsequent transport, dilution, or chemical evolution of the exhaust plume is not simulated. While this study establishes where exhaust is introduced into the atmosphere, it does not assess where it ultimately resides or how it transforms. Especially in the high atmosphere the point of emission and the final point where the exhaust ceases independent motion relative to the surrounding atmosphere, could differ significantly.

One central limitation of this study is that it quantifies the amount and composition of rocket exhaust but does not assess the environmental effects of these emissions. Limited analysis is performed on the potential qualitative climate and ozone impacts of design decisions. Some trends, like the central role of black carbon start to materialize in research [5, 9, 20], but the overall impact and the individual impact of specific species remains highly debated [5, 8, 9, 20, 21]. As such, the results should be interpreted as a physical inventory of exhaust, not as a direct evaluation of their environmental impact.

Without a quantified assessment of the launch emission impact, it remains unclear how their environmental impact compares to other life cycle processes, such as fuel production or vehicle manufacturing. This knowledge gap limits the ability to make informed EcoDesign decisions. For instance, in the case of reusable stages, it is still uncertain whether the increased propellant consumption and associated exhaust—identified in this study and in the ENTRAIN analyses [1–4, 12, 13]—offset the environmental benefits gained from producing fewer stages. The choice of propellant may also play a critical role, as increased exhaust mass may have less environmental significance for hydrogen-fuelled systems than for hydrocarbon-based launchers [21].

DOI: 10.13009/EUCASS2025-495

6 Conclusion

This study presents a comprehensive assessment of the launch exhaust generated by various reusable and expendable launcher configurations investigated in the ENTRAIN study. Using consistent mission objectives, modeling tools, and design assumptions, the analysis isolates the influence of engine cycle, propellant choice, and recovery method on the total mass, distribution, and composition of exhaust products during ascent and, where applicable, booster return.

Propellant choice was identified as the most influential factor affecting the total exhaust mass and its chemical composition LOX-LH_2 launchers produce the lowest exhaust, consisting almost entirely of water vapor, while LOX-RP-1 configurations result in the highest total exhaust and largest emissions of carbon-based compounds, including elemental carbon. LOX-LCH_4 configurations, show behaviour close to RP-1 systems in terms of total exhaust quantity and composition, only the exhaust of elemental carbon is reduced by one order of magnitude. The hybrid configurations, with LOX-LCH_4 in the first stage and LOX-LH_2 in the second stage, achieve a 50% reduction of the total exhaust compared to full methane launchers, as the lighter upper stage allows for a considerably lower total fuel mass.

Engine cycle selection also plays a significant role. Configurations with staged combustion engines consistently yield lower total exhaust compared to configurations with gas generator engines due to their higher specific impulse. For hydrocarbon systems, this exhaust mass difference is with up to 31% particularly pronounced and gas generator engines introducing additional exhaust products such as unburned methane and elemental carbon.

The recovery method impacts the total amount and vertical distribution of exhaust. While expendable configurations produce the lowest total exhaust due to the absence of return manoeuvres and recovery hardware- vertical down range landing configurations show the highest exhaust mass. This increase stems from the additional Δv required for reentry and landing burns, along with added dry mass for landing systems. These return manoeuvres generate distinct exhaust peaks in the lower meso- and upper stratosphere and at ground level. In-air capturing avoids descent propulsion but adds structural mass, resulting in an intermediate total exhaust and a more concentrated altitude distribution, due to a shallower ascent trajectory.

This study provides a detailed exhaust inventory for reusable launch systems, developed under consistent and comparable conditions. From DLR's perspective, these results offer a foundation for research into the broader environmental implications of launcher emissions. However, three key challenges remain. First, a more comprehensive understanding of plume chemistry and dynamics is needed to accurately link exhaust to atmospheric emissions. Second, the environmental impact of these emissions must be systematically quantified. Third, these findings must be integrated into a holistic life cycle sustainability assessment of launch systems. Such an assesment enables the identification of environmental hot spots across the launcher life cycle and supports targeted mitigation strategies through EcoDesign. To address these environmental, social, and economic challenges in an integrated manner, DLR is launching the S3D project, which aims to incorporate sustainability considerations into the early design phases of future space transportation systems and space missions.

DOI: 10.13009/EUCASS2025-495

References

[1] J. Wilken, M. Herberhold, and M. Sippel, "Options for future European reusable booster stages: evaluation and comparison of VTHL and VTVL costs," *CEAS Space J*, vol. 17, no. 1, pp. 177–198, 2025, doi: 10.1007/s12567-024-00577-5.

[2] J. Wilken and S. Stappert, "Comparative analysis of European vertical landing reusable first stage concepts," *CEAS Space J*, vol. 17, no. 1, pp. 113–130, 2025, doi: 10.1007/s12567-024-00549-9.

[3] L. Bussler, I. Dietlein, and M. Sippel, "Comparative analyses of European horizontal-landing reusable first stage concepts," *CEAS Space J*, vol. 17, no. 1, pp. 131–154, 2025, doi: 10.1007/s12567-024-00572-w.

[4] I. Dietlein, L. Bussler, S. Stappert, J. Wilken, and M. Sippel, "Overview of system study on recovery methods for reusable first stages of future European launchers," *CEAS Space J*, vol. 17, no. 1, pp. 71–88, 2025, doi: 10.1007/s12567-024-00557-9.

[5] R. G. Ryan, E. A. Marais, C. J. Balhatchet, and S. D. Eastham, "Impact of Rocket Launch and Space Debris Air Pollutant Emissions on Stratospheric Ozone and Global Climate," *Earth's future*, vol. 10, no. 6, e2021EF002612, 2022, doi: 10.1029/2021EF002612.

[6] J.-S. Fischer *et al.*, "A Pathway for Closing the Knowledge Gaps for a Comprehensive Life Cycle Assessment and Ecodesign of Space Transportation Systems - Results of the 3rd Workshop on Life Cycle Assessment of Space Transportation Systems," 2024.

[7] Michael M. James *et al.*, *Commercial Space Vehicle Emissions Modeling*. Washington, D.C.: Transportation Research Board, 2021.

[8] C. M. Maloney, R. W. Portmann, M. N. Ross, and K. H. Rosenlof, "Investigating the Potential Atmospheric Accumulation and Radiative Impact of the Coming Increase in Satellite Reentry Frequency," *JGR Atmospheres*, vol. 130, no. 6, 2025, doi: 10.1029/2024JD042442.

[9] C. M. Maloney, R. W. Portmann, M. N. Ross, and K. H. Rosenlof, "The Climate and Ozone Impacts of Black Carbon Emissions From Global Rocket Launches," *JGR Atmospheres*, vol. 127, no. 12, 2022, doi: 10.1029/2021JD036373.

[10] J.-S. Fischer and S. Fasoulas, "Assessment of Launch and Re-Entry Emissions of Space Transportation Systems and Their Environmental Impact," in *IAF Space Transportation Solutions and Innovations Symposium*, Milan, Italy, 2024, pp. 756–766.

[11] Space Exploration Technologies Corp, "Falcon Users's Guide," 2021. [Online]. Available: https://www.spacex.com/media/falcon-users-guide-2021-09.pdf

[12] M. Sippel and J. Wilken, "Selection of propulsion characteristics for systematic assessment of future European RLV-options," *CEAS Space J*, vol. 17, no. 1, pp. 89–111, 2025, doi: 10.1007/s12567-024-00564-w.

[13] S. Stappert, I. Dietlein, J. Wilken, L. Bussler, and M. Sippel, "Options for future European reusable booster stages: evaluation and comparison of VTHL and VTVL return methods," *CEAS Space J*, vol. 17, no. 1, pp. 155–175, 2025, doi: 10.1007/s12567-024-00571-x.

[14] Thomas Bellier, Joseph Morlier, Cees Bil, Annafederica Urbano, and Adrian Pudsey, "INTEGRATION OF LIFE CYCLE ASSESSMENT METHODOLOGY AS AN ENVIRONMENT DISCIPLINE MODULE IN MULTIDISCIPLINARY ANALYSIS AND OPTIMIZATION FRAMEWORK,"

[15] H. Kayal, "Aufbau eines vereinfachten Simulationsmodells für den Bahnaufstieg in der Großkreisebene," 1993. [Online]. Available: https://elib.dlr.de/23152/

[16] A. Ponomarenko, "RPA: Design Tool for Liquid Rocket Engine Analysis," 2010. [Online]. Available: https://rocket-propulsion.com/publications.htm

[17] G. P. Sutton, *Rocket Propulsion Elements*, 9th ed. New York: John Wiley & Sons Incorporated, 2017. [Online]. Available: http://gbv.eblib.com/patron/FullRecord.aspx?p=4756773

[18] A. Ponomarenko, "Assessment of Delivered Performance of Thrust Chambers," 2013. [Online]. Available: https://rocket-propulsion.com/publications.htm

[19] C. R. Barker, E. A. Marais, and J. C. McDowell, "Global 3D rocket launch and re-entry air pollutant and CO2 emissions at the onset of the megaconstellation era," *Scientific data*, vol. 11, no. 1, p. 1079, 2024, doi: 10.1038/s41597-024-03910-z.

[20] M. N. Ross and P. M. Sheaffer, "Radiative forcing caused by rocket engine emissions," *Earth's future*, vol. 2, no. 4, pp. 177–196, 2014, doi: 10.1002/2013EF000160.

[21] E. J. L. Larson, R. W. Portmann, K. H. Rosenlof, D. W. Fahey, J. S. Daniel, and M. N. Ross, "Global atmospheric response to emissions from a proposed reusable space launch system," *Earth's future*, vol. 5, no. 1, pp. 37–48, 2017, doi: 10.1002/2016EF000399.

[22] M. Ross, M. Mills, and D. Toohey, "Potential climate impact of black carbon emitted by rockets," *Geophysical Research Letters*, vol. 37, no. 24, 2010, doi: 10.1029/2010GL044548.

DOI: 10.13009/EUCASS2025-495

A. Appendix A: Performance and mass parameter of ENTRAIN launchers

Table 6: Performance and mass parameter of selected expendable ENTRAIN launchers [1]

Fuel	**-**	**LH_2**		**LCH_4**		**HYBRID**
Engine cycle	-	GG	SC	GG	SC	GG
2^{nd} stage Δv	[km/s]	7	7	7	7	7
Staging category	-	Med	Med	Med	Med	Med
Designation	-	EL HH GG Med	EL HH SC Med	EL CC GG Med	EL CC SC Med	EL CH SC Med
1^{st} stage Propellant loading	[t]	234	192	580	450	315
2^{nd} stage Propellant loading	[t]	75	64	148	125	70
Payload to GTO	[t]	7.57	7.55	7.41	7.54	7.51
Payload to SSO	[t]	15	13.8	18.5	17.5	14.6
SSO GLOM	[t]	362	297	810	637	419

DOI: 10.13009/EUCASS2025-495

Table 7: Performance and mass parameter of selected vertical landing ENTRAIN launchers [2]

Fuel	**-**	**LH_2**		**LCH_4**		**KK**	**HYBRID**
Engine cycle	-	GG	SC	GG	SC	GG	GG
2nd stage Δv	[km/s]	7	7	7	7	7	7
Staging category	-	Med	Med	Med	Med	Med	Med
Designation	-	VL HH GG Med	VL HH SC Med	VL CC GG Med	VL CC SC Med	VL KK GG Med	VL CH SC Med
1st stage Propellant loading	[t]	305	245	850	625	928	432
2nd stage Propellant loading	[t]	75	64	148	125	169	70
Payload to GTO	[t]	7.49	7.46	7.45	7.62	7.64	7.47
Payload to SSO	[t]	14.9	13.5	18.1	16.9	14.4	18.5
Payload to SSO with RTLS	[t]	10.3	9.8	9.6	10.4	11.0	9.7
SSO GLOM	[t]	455	374	1119	845	1164	577

Table 8: Performance and mass parameter of selected horizontal landing ENTRAIN launchers [3]

Fuel	**-**	**LH_2**		**LCH_4**	**KK**
Engine cycle	-	GG	SC	GG	GG
2nd stage Δv	[km/s]	7	7	7	7
Staging category	-	Med	Med	Med	Med
Designation	-	HL HH GG Med	HL HH SC Med	HL CC GG Med	HL KK GG Med
1st stage Propellant loading	[t]	205	245	575	642
2nd stage Propellant loading	[t]	64	75	150	152
Payload to GTO	[t]	7.52	7.59	7.43	7.58
Payload to SSO	[t]	14.4	14.2	17.9	18.1
SSO GLOM	[t]	391	335	826	880